Proceedings of the ASME 2018 International Design Engineering Technical Conferences and Computers and Information in Engineering Conference IDETC/CIE 2018 August 26-29, 2018, Quebec City, Quebec, Canada

DETC2018-85703

SENSORY GLOVE FOR DYNAMIC HAND PROPRIOCEPTION AND TACTILE SENSING

John C.S. McCaw, Michelle C. Yuen*
School of Mechanical Engineering
Purdue University
West Lafayette, Indiana 47907
Email: {mccaw, yuenm}@purdue.edu

Rebecca Kramer-Bottiglio*
School of Engineering and Applied Science
Yale University
New Haven, Connecticut 06510
Email: rebecca.kramer@yale.edu

ABSTRACT

The fields of soft robotics and soft electronics have introduced novel technologies for tracking dynamic pose of the human body. These new flexible sensors use material softness and elasticity to allow for high conformability, low risk of injury or discomfort, and ease of integration into other flexible materials such as clothing. Here, we present a glove embedded with soft capacitive strain sensors for measuring finger bending and fingertip pressure, while leveraging low-cost components. Previous capacitive sensing approaches have shown limitations in dimensional scalability of the sensor geometry and system-level scalability of sensors, wiring, and networking methods. We overcome these previous limitations by using sensors with novel geometry and leverage I^2C communication protocol to reduce the quantity of interfacing wires to four, even for sensor counts on the order of 10^3. We show that the sensory glove is able to capture the salient features of hand proprioception by sensing the presence and continuous intensity of touch and finger curvature. Finally, we demonstrate the application of this glove towards the recognition of the letters comprising the American Manual Alphabet, which is used to augment the American Sign Language, and utilize the glove to perform a teleoperation task.

1 Introduction

Hand proprioception and tactile sensing offer a wide variety of applications in human-computer interaction, including gesture-based control for teleoperation, state reconstruction of the hand in virtual and augmented reality, and gesture-based language input. With 27 degrees of freedom, the human hand can serve as a much richer input device relative to devices like joysticks, mice, and keyboards [1]. While many degrees of freedom enables the high dexterity of human hands, it is also a complex mechanical system that is difficult to resolve without compromising the natural biomechanics of hand motion. Ideally, a hand proprioception and tactile sensing system would be able to measure the state of the fingers without interfering with their range or dynamics of finger motion. Furthermore, when considering use of such a device, the overall system would ideally be as physically discrete as possible, so as to be imperceptible to the user.

Developments in soft robotics and high-strain flexible technologies have provided a variety of methods for hand proprioception and tactile sensing, which fit into five primary categories: resistive strain sensors [2–8], capacitive strain sensors [9–11], optical sensors [12–14], inertial measurement units (IMUs) [15–17], and visual motion capture systems [18, 19]. One of our goals in this work was to minimize the effect of the wearable device on natural hand biomechanics. As such, since IMUs are not a 'soft' component, they are not considered herein.

Currently, motion capture systems provide the most accurate joint angle data with a high degree of repeatability, with recent work consistently achieving $<1\%$ error [18]. However, the space limitations and obstructions incurred by using motion capture cameras make it not viable for use in open environments. Additionally, the high cost of motion capture systems makes them

*M.C. Yuen is also affiliated with Yale University.

inviable in all but a few specialized, high-value applications.

Optical sensors have been shown in sensing gloves to determine joint angle with high degrees of sensitivity, and are not susceptible to electromagnetic interference [12–14]. However, due to this sensor type operating on the basis of light intensity through a fiber-optic cable, they are highly susceptible to damage and require specialized electronics.

Soft strain and pressure sensors utilizing resistive [2–6] and capacitive [9–11] sensing modalities have been demonstrated in a variety of forms to measure finger bending and contact pressure. Both of these sensing methods rely upon direct deformation of the soft material comprising the sensor body to change their measured resistance or capacitance. Compared to the other sensing methods, resistive and capacitive strain sensors provide the benefit of simple incorporation into an electronic circuit. Deformation-sensitive resistors need only be placed in a voltage divider circuit to provide meaningful output, and similarly, deformation-sensitive capacitors may be placed in a circuit measured with the time constant of a first order system.

A key difference between resistive and capacitive strain sensors is the dependence on material properties: resistive sensors are sensitive to changes in the geometry and the resistivity of a resistive element, while capacitive sensors measure changes in bulk sensor geometry. As a result, capacitive sensors are less susceptible to material degradation that can result in long-term signal drift in resistive sensors, with the added advantage that material constraints in resistivity are no longer a primary concern. Furthermore, while many issues with material degradation and device failure in high-deformation resistive sensors can be mitigated with the use of liquid metals and ionic liquids, these sensors are difficult to fabricate and are often susceptible to failure at the poor physical interface between rigid wires and liquid conductors.

One concern with hand proprioception is the number of wires required to capture signals from a large number of sensors required to capture the dynamics of the hand. Traditional capacitive sensing devices require three lines to operate: ground, power, and signal. Other methods of sensing, such as optical methods, require many more wires [14]. To reduce the number of wires, researchers have incorporated an I^2C communication protocol to transmit a binary on-off value back to a central processor [9].

In this work, we present a high-resolution, propioceptive glove functionalized with soft, capacitive strain sensors. The number of wires on the glove are reduced by implementing the I^2C communication protocol. the work presented here also extends our prior work [20] by showing that the geometry of the elastomer-based strain sensors can still operate well when scaled to a very small size and operating in close proximity to charged bodies (human bodies). Similar to the prior work by Seehra, *et al.* [17], our glove and sensors are fabricated from low-cost materials. Finally, we demonstrate sign language capture and teleoperation using this glove.

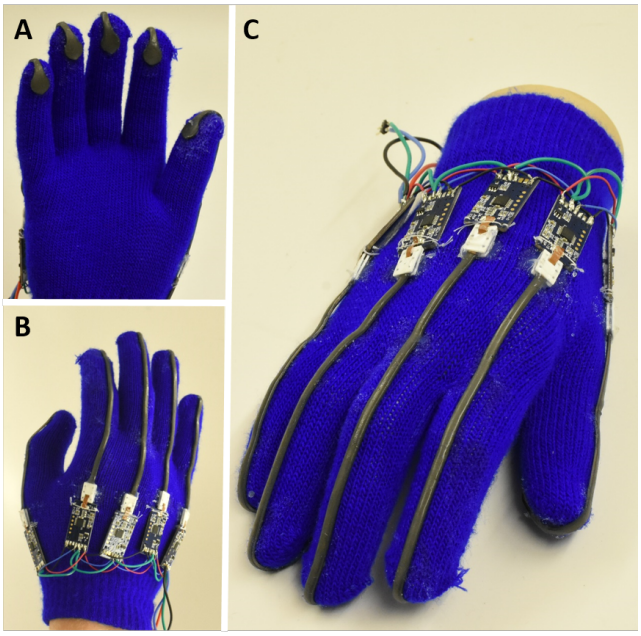

FIGURE 1. Images of the sensory glove. (A) Glove worn on a hand, seen from the ventral plane, showing the pressure-sensitive fingertips, (B) the dorsal plane, showing the length of the sensor responsive to bending the fingers, and (C) a perspective angle on a mannequin hand.

2 Materials and Manufacture

2.1 Sensor Fabrication

A schematic of the sensor fabrication is shown in Figure 2. The sensors presented here are composed of platinum-cure silicone elastomer (Dragon Skin 10 Slow, Smooth-On) and a silicone elastomer and expanded graphite composite material. The sensors are constructed as parallel-plate capacitors, following the same procedure for film-based sensors as described in [20]. In brief, to manufacture the conductive electrode layers, expanded intercalated graphite (EIG) (Expandable Graphite Flakes, Sigma-Aldrich) was incorporated into the silicone elastomer at a loading of 10wt% with the aid of an organic solvent (Cyclohexane, VWR Analytical). The material was cast into a film by rod-coating (1/2 in. Acme Threaded Rod, McMaster-Carr). We allowed the solvent to evaporate and the elastomer to cure. The dielectric layer was constructed by preparing unmodified silicone elastomer and rod-coating over the electrode layer in the same fashion. Before the dielectric layer had fully cured, the assembly was folded in half resulting in a four layer structure: electrode-dielectric-dielectric-electrode.

The individual sensors were laser-cut from the larger sheet (30W CO_2 laser; Universal Laser Systems VLS 2.30) using a

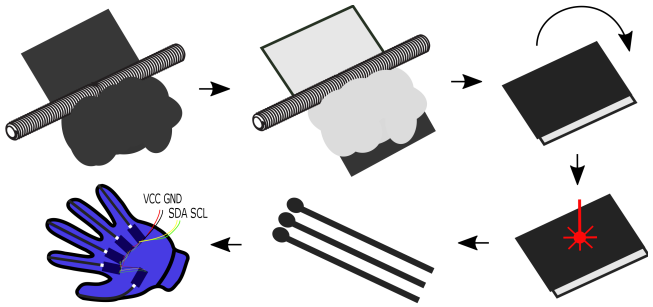

FIGURE 2. Fabrication procedure. (Top left) Expanded intercalated graphite and silicone elastomer composite is rod-coated into a film. (Top middle) After curing, silicone elastomer is rod-coated on top of the composite film. (Top right) The film is folded over onto itself to form the capacitor structure when the silicone elastomer has cured to a tacky stage. (Bottom right) The film is laser cut into the sensor patterns. (Bottom middle) The sensors are cleaned, interfaces are attached, and the sensors are dipped in silicone elastomer to form a thin insulating coat. (Bottom left) The sensors and custom microprocessor boards are glued on the glove using silicone elastomer as adhesive. The four I^2C wires, VCC (power), GND (ground), SDA (digital data), and SCL (digital clock), extend from the final sensor to the microcontroller (not pictured).

custom pattern designed for each finger's length. To interface with the capacitance measurement electronics, copper contacts were attached to each conductive side with laser-cut polystyrene tabs held together with thread, shown in Figure 1B-C. The entire assembly was coated in silicone elastomer for environmental protection by dipping the sensors into the uncured elastomer and allowing it to flow by gravity until cured.

2.2 Glove Assembly

The polystyrene tabs, shown in Figure 1A, were glued to the glove with silicone elastomer, and the sensor body was pre-strained to 10% before being fixed down with more silicone elastomer at the copper contacts, halfway along their length, and at the fingertips. The custom microprocessor boards used to measure the capacitances of the sensors (reported in [20]) were fixed to the glove with cotton thread and wired in parallel to form the I^2C bus. Here, the I^2C master was implemented using an Arduino Pro Mini microcontroller (Adafruit), which sends the data over UART to a computer running a custom Python script. The total cost of the materials and electronics involved was less than $40USD at the time of writing.

2.3 Electronics Operation

The individual custom microprocessor boards operate on the basis of a fixed-time charging circuit. The positive side of the soft capacitive strain sensor is allowed to charge for a fixed time, using the internal clock of the microprocessor. After charging the capacitive sensor, the internal clock is used to record the time it takes for the capacitor to discharge to a fixed voltage value, dictated by the component values in the circuit. This time is stored in I^2C accessible memory, and the process continues whenever the microprocessor is powered on.

This I^2C Protocol is well documented, though a brief overview of how it is used in this work is included for readers unfamiliar with its operation. The master device, which in this case is the Arduino microcontroller, uses the communications lines to send out the address of the slave with which it wishes to communicate. Following this, the master sends the memory address (on the slave) it wants, which is followed by the slave sending this information to the master. Because this system uses 7-bit addresses, there are 128 possible sensors, though I^2C systems with 10-bit addresses (1024 addresses) are also possible.

3 Signal Processing

During operation, we applied a simple exponential filter to the data passing through the microprocessor with a decay rate, $\alpha = 0.2$. Thus, the value recorded and reported here is $s_t = \alpha x_t + (1-\alpha)s_{t-1}$, where x_t is the current, raw sensor reading, and s_{t-1} is the previous filtered value. This filtering method is memory-light (only a single value per sensor is held in memory at any one time), which is beneficial for wearable systems wherein the goal is to minimize the footprint of computing hardware and power supply. Additionally, for further clarity in reporting, a low-pass FIR filter with Kaiser Window was applied after data collection, having a passband frequency of 0.2 Hz and a stopband frequency of 20 Hz attenuated by 20 dB. In the plots presented in this paper, we normalized the readings by dividing the reading by the initial, unloaded sensor value across all tests.

4 Sensor Response Characterization

We characterized the sensor response to finger curvature and pressure at the finger pads, and furthermore, demonstrated that individual sensor responses are independent from one another (*i.e.*, we observe no electrical coupling despite the implementation of the the communication protocol and the close proximity of the sensors). The mechanical response of these sensors to strain was previously characterized by White, et al. [20], where the authors found the sensors to have a linear electrical response to applied strain, to have no observable change in function over 1000 cycles and to remain functional through 100,000 cycles. Further, the sensors are able to function through 250% strain and return to normal function. Because the behavior of the standalone sensors have been thoroughly studied, we have focused on characterizing the glove as a whole system, rather than characterizing individual sensors.

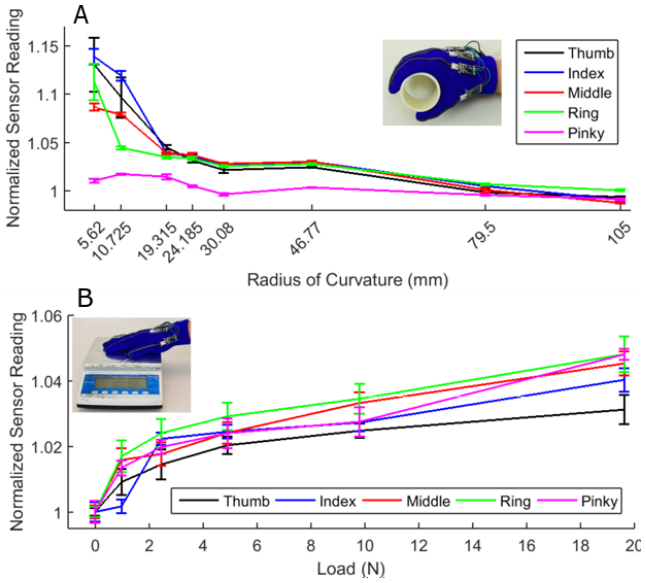

FIGURE 3. (A) Plots showing the radius of curvature and (B) pressure response characterization of the glove. All error bars represent mean and 95% confidence bounds calculated from 100 readings at each measurement point. Photo insets show an example of the hand positions in each experimental setup.

4.1 Curvature Response

Curvature response was determined by grasping cylinders of different diameters, while minimizing pressure on the fingertips (Figure 3A). We sampled the sensors 100 times at approximately 500 Hz for each radius of curvature. The thumb was positioned in the opposite direction of the fingers except for the largest two diameters, for which it was necessary to position the thumb parallel to the fingers. All fingers had similar levels of response to the applied curvature. At the largest diameters, there is little change in the sensor readings because the fingers lay nearly flat. With the exception of the smallest two radii of curvature, the confidence bounds for all fingers at each remaining measurement point are similarly narrow, indicating that the resolution with which we can distinguish different curvatures remains consistent. Using this data, one can correlate curvature of the fingers to the sensor reading.

4.2 Pressure Response

The pressure response of the finger pads, shown in Figure 3B, was determined by applying a force on a scale with the hand and sampling the sensors 100 times at approximately 500 Hz. The plot shows the sensor reading (mean and 95% confidence bound) for each finger as a function of applied load. We found that all the fingers displayed similar levels of response to the same load. Furthermore, We note the sharper increase at smaller loads, and attribute this to the effect of the sensor contact with the scale, in addition to the deformation due to applied load. Contact with objects typically results in an increase in capacitance, regardless of making a conductive connection. The polarizability of material near the sensor increases the measured capacitance. As the load increases, the contact between the sensor and the scale is the same as when smaller amounts of load are applied.

We note here that it is not currently possible for this system to distinguish between finger curvature and applied pressure - both result in an increase in the sensor reading. This is because the current sensor construction consists of a single soft capacitive stretch sensor that begins before the metacarpophalangeal joint and wraps around the tip of the finger, terminating on the pad. Future iterations may separate the sensor into two individual sensors in order to measure both values simultaneously.

4.3 De-coupled Response

Finally, we observed the de-coupled nature of the sensors, aside from natural biomechanical coupling of the third, fourth, and fifth fingers. Figure 4 shows the bending of individual fingers in succession, and their corresponding sensor output as a function of time. Some of the regions in this plot show a large-magnitude activation alongside smaller magnitude sensor activations on proximate fingers, due to their biomechanical coupling. This demonstration shows that the individual sensors are electrically de-coupled, despite their mutual proximity and proximity to the communication lines.

5 Applications

The developed glove shows promise with applications related to gesture-based proprioception, such as control of video games, gesture-based user interfaces, and capture of manual al-

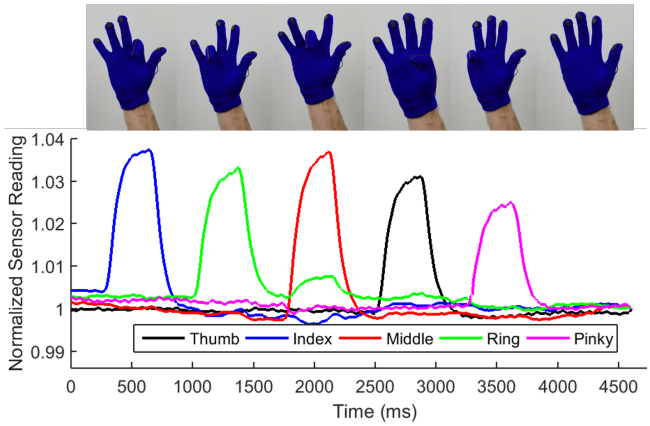

FIGURE 4. Real-time output of the sensor glove showing individual finger response. The images above the plot show which finger is being bent at each region.

phabet, sign language or natural language gestures. The Peregrine Glove is an example of a glove-based video game controller, but is limited to on/off switches made of conductive traces on the glove [21]. A continuous, analog approach, such as the glove presented herein, allows the user to further control their actions beyond on-off switching. For example, a user could send the game an instruction of a direction and velocity in that direction to move a character. Alternatively, different degrees of joint angle may be mapped to discrete key codes so multiple, traditional keystrokes may be logged per finger.

The signals from the glove can also be used to map gestures to text to allow for sign language communication without a tele-interpreter, or similar gesture-to-text or gesture-to-speech tools. Here, American Sign Language (ASL) will be used as an example since it can be used to communicate text and abstract ideas with a single hand, such as the American Manual Alphabet and full words or phrases. To exemplify each, a spelling example and a single-gesture word are presented. We then demonstrate the application of this glove towards performing a teleoperation task by controlling various joints of a robotic arm.

5.1 Capture of American Sign Language

To demonstrate the application of this glove to American Sign Language, we signed two common categories of signs (Figure 5). One component of American Sign Language is the American Manual Alphabet, which consists of 26 signs that correspond to the 26 letters of the English Alphabet. In Figure 5A, the operator signs the letters spelling 'BOILERUP'. It is apparent from the plot that the letters here can be clearly distinguished from one another using the five sensors on the glove. It is important to clarify that the set of 26 characters cannot be fully determined by a strain sensor across each finger; some characters are spatial rotations of others, such as the difference between 'H' and 'U', and others have the similar finger curvatures such as 'O' and 'E' but have different orientations relative to the hand. Integration of multiple strain sensors per finger to further clarify location of finger curvature, as well as an additional sensor across the wrist to register hand orientation, would allow for the full character set to be classified.

A second major component of American Sign Language is non-alpha-numeric gestures and positions that represent words and phrases, and are often dependent on the order, speed, and timing of the motions. To demonstrate the ability of the sensory glove reported here, a common ASL sign was made that represents the phrase, 'I Love You,' shown in Figure 5B.

5.2 Teleoperation

We demonstrated the application of the glove toward teleoperation (Figure 6). The four fingers of the sensory glove were each used to independently control a different degree of freedom (Row 1 in Figure 6) on a robotic arm with servos at each of the

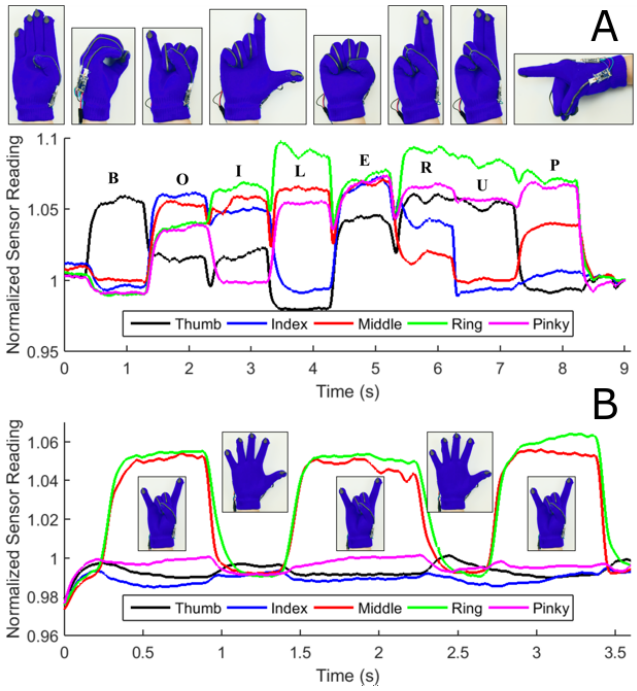

FIGURE 5. Demonstration of American Sign Language recognition. The plots show the normalized sensor values of all fingers with respect to time. (A) Individual letters to spell out 'BOILERUP' are demonstrated, along with the phrase 'I Love You', followed by an open hand, and then repeated two more times (B).

joints. The index finger and ring finger sensor measurements were mapped linearly to two of the joints in the robot arm. The middle finger and pinky finger sensor measurements were used to switch between two motor positions. The sensors were sampled at approximately 500Hz and an exponential filter was applied with a decay rate $\alpha = 0.97$. Using all four fingers, we controlled these four degrees of freedom of the robotic arm in performing a pick-and-place operation, followed by a re-positioning of the object. This teleoperation task shows the potential of using the glove as a continuous input device. Furthermore, the teleoperation task demonstrates that only a minimal amount of signal processing is needed to use the data from the glove. The observed stability and robustness of the sensors reduces the amount of computing hardware and power supplies, thus reducing rigid materials (*i.e.* PCBs) on the body in wearable applications.

6 Conclusions and Future Work

The glove presented in this paper demonstrates the application of soft, flexible sensors to hand proprioception and tactile sensing. By using soft and compliant materials for both the glove and sensors, the resulting glove accommodates the wide variability in hand shape, meeting a key criterion in Design for

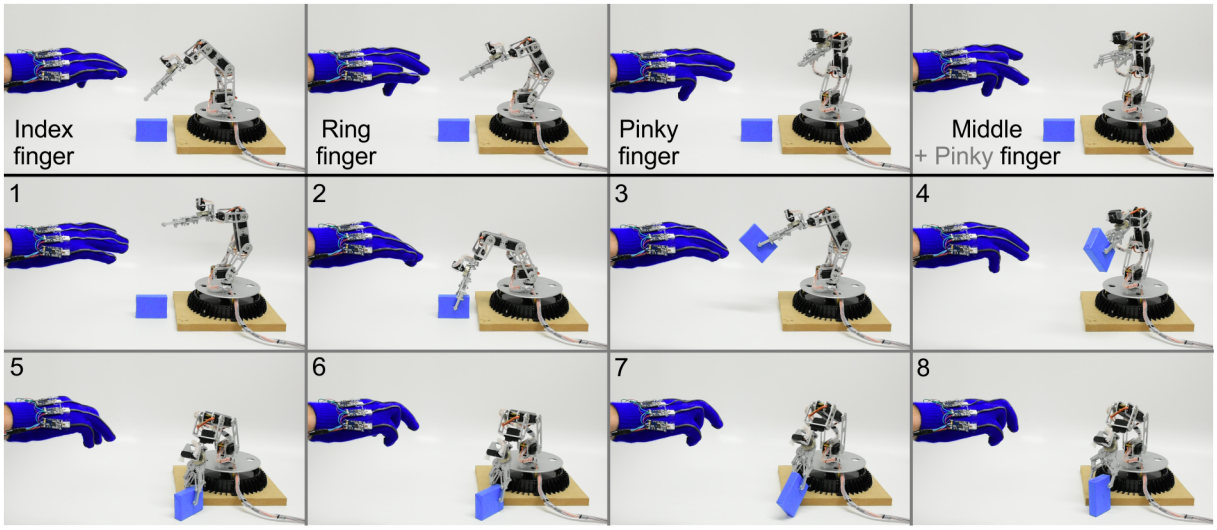

FIGURE 6. Teleoperation demonstration. Box 1 shows the hand and robotic arm in its initial position. The top row shows the individual joints controlled by each finger. The index and ring fingers control their respective joints in a continuous manner. The pinky and middle fingers trigger a change between two motor positions dependent on the sensor value passing a threshold value. The bottom two rows show a sequence in the teleoperation task: the robot arm reaches down and picks up a box, rotates to a new position, deposits the box, and then re-positions the box.

Human Variability (DfHV). The sensors are constructed from low-cost materials, and the fabrication process allows for facile customization of sensor design. Use of I^2C protocol reduces the number of control wires needed, while also providing a low-cost alternative. While this glove measures fewer degrees of freedom than are present in the human hand, the information provided allows the finger curvature to be determined, which may be used in a variety of applications ranging from human-computer interfaces to sign language capture. Additionally, the pressure-sensitive finger pads provide another mode of input, alongside finger curvature. Finally, as self-reported by the authors, finger and hand motions with the functionalized glove were indistinguishable from an unmodified glove, achieving our goal of not restricting mechanical motion of the hand. While the current glove uses sensors that cannot distinguish between pressure and curvature, the two modes can be sensed using separate sensors as desired for a given application.

In future iterations of wearable devices enabled by capacitive strain sensing, a more advanced electrical model of the sensor is needed. As the geometry decreases past what is presented here, the linear relationship between capacitance and strain will no longer accurately predict the state (strain) of the system because the change in impedance of the conductive EIG composite electrodes under strain is expected to have a more dominant effect on the sensor reading. Another area of focus in the future is to reduce the size of the custom microprocessor boards used to interrogate the sensors, to further increase the conformability of the system. Finally, the addition of a shielding layer of conductive composite surrounding the sensors would reduce the impact of spurious signals from the ambient environment, and would reduce the amount of filtering required for the signal, paving the way for a more immediate, real-time system response.

7 Acknowledgements

The authors thank Dr. Edward L. White and Dylan S. Shah for assistance in electronic design and signal processing, as well as for general advice during this project, and R. Adam Bilodeau for assisting with photography. JCSM and this work were supported by a grant from Intel Corporation. MCY is supported by the National Science Foundation Graduate Research Fellowship (Grant DGE-1333468).

REFERENCES

[1] Y. Wu and T. S. Huang, "Capturing articulated human hand motion: a divide-and-conquer approach," in *Proceedings of the Seventh IEEE International Conference on Computer Vision*, vol. 1, 1999, pp. 606–611 vol.1.

[2] R. K. Kramer, C. Majidi, R. Sahai, and R. J. Wood, "Soft curvature sensors for joint angle proprioception," in *Intelligent Robots and Systems (IROS), 2011 IEEE/RSJ International Conference on*, 2011, pp. 1919–1926.

[3] T. F. OConnor, M. E. Fach, R. Miller, S. E. Root, P. P. Mercier, and D. J. Lipomi, "The language of glove: Wireless gesture decoder with low-power and stretchable hybrid electronics," *PloS one*, vol. 12, no. 7, p. e0179766, 2017.

[4] M. Amjadi, A. Pichitpajongkit, S. Lee, S. Ryu, and I. Park,

"Highly Stretchable and Sensitive Strain Sensor Based on Silver NanowireElastomer Nanocomposite," *ACS Nano*, vol. 8, no. 5, pp. 5154–5163, May 2014.

[5] F. L. Hammond, Y. Mengüç, and R. J. Wood, "Toward a modular soft sensor-embedded glove for human hand motion and tactile pressure measurement," in *Intelligent Robots and Systems (IROS 2014), 2014 IEEE/RSJ International Conference on*. IEEE, 2014, pp. 4000–4007.

[6] A. P. Gerratt, H. O. Michaud, and S. P. Lacour, "Elastomeric Electronic Skin for Prosthetic Tactile Sensation," *Adv. Funct. Mater.*, vol. 25, no. 15, pp. 2287–2295, Apr. 2015.

[7] H. O. Michaud, J. Teixidor, and S. P. Lacour, "Soft flexion sensors integrating strechable metal conductors on a silicone substrate for smart glove applications," in *2015 28th IEEE International Conference on Micro Electro Mechanical Systems (MEMS)*, Jan. 2015, pp. 760–763.

[8] H. O. Michaud, L. Dejace, S. d. M. Mulatier, and S. P. Lacour, "Design and functional evaluation of an epidermal strain sensing system for hand tracking," in *2016 IEEE/RSJ International Conference on Intelligent Robots and Systems (IROS)*, Oct. 2016, pp. 3186–3191.

[9] M. D. Bartlett, E. J. Markvicka, and C. Majidi, "Rapid Fabrication of Soft, Multilayered Electronics for Wearable Biomonitoring," *Advanced Functional Materials*, vol. 26, no. 46, pp. 8496–8504, Dec. 2016.

[10] A. Atalay, V. Sanchez, O. Atalay, D. M. Vogt, F. Haufe, R. J. Wood, and C. J. Walsh, "Batch Fabrication of Customizable Silicone-Textile Composite Capacitive Strain Sensors for Human Motion Tracking," *Adv. Mater. Technol.*, 2017.

[11] A. P. Gerratt, N. Sommer, S. P. Lacour, and A. Billard, "Stretchable capacitive tactile skin on humanoid robot fingers - First experiments and results," in *2014 IEEE-RAS International Conference on Humanoid Robots*, Nov. 2014, pp. 238–245.

[12] M. Nishiyama and K. Watanabe, "Wearable Sensing Glove With Embedded Hetero-Core Fiber-Optic Nerves for Unconstrained Hand Motion Capture," *IEEE Transactions on Instrumentation and Measurement*, vol. 58, no. 12, pp. 3995–4000, Dec. 2009.

[13] A. F. d. Silva, A. F. Goncalves, P. M. Mendes, and J. H. Correia, "FBG Sensing Glove for Monitoring Hand Posture," *IEEE Sensors Journal*, vol. 11, no. 10, pp. 2442–2448, Oct. 2011.

[14] H. Zhao, K. OBrien, S. Li, and R. F. Shepherd, "Optoelectronically innervated soft prosthetic hand via stretchable optical waveguides," *Science Robotics*, vol. 1, no. 1, p. eaai7529, Dec. 2016.

[15] T. L. Baldi, S. Scheggi, L. Meli, M. Mohammadi, and D. Prattichizzo, "GESTO: A Glove for Enhanced Sensing and Touching Based on Inertial and Magnetic Sensors for Hand Tracking and Cutaneous Feedback," *IEEE Transactions on Human-Machine Systems*, vol. PP, no. 99, pp. 1–11, 2017.

[16] H. Liu, X. Xie, M. Millar, M. Edmonds, F. Gao, Y. Zhu, V. J. Santos, B. Rothrock, and S.-C. Zhu, "A Glove-based System for Studying Hand-Object Manipulation via Joint Pose and Force Sensing."

[17] J. S. Seehra, A. Verma, and K. Ramani, "ChiroBot: modularrobotic manipulation via spatial hand gestures." ACM Press, 2014, pp. 209–212.

[18] X. Wei, P. Zhang, and J. Chai, "Accurate realtime full-body motion capture using a single depth camera," *ACM Transactions on Graphics*, vol. 31, no. 6, p. 1, Nov. 2012.

[19] P. Vicente, L. Jamone, and A. Bernardino, "Robotic Hand Pose Estimation Based on Stereo Vision and GPU-enabled Internal Graphical Simulation," *Journal of Intelligent & Robotic Systems*, vol. 83, no. 3-4, pp. 339–358, Sep. 2016.

[20] E. L. White, M. C. Yuen, J. C. Case, and R. K. Kramer, "Low-Cost, Facile, and Scalable Manufacturing of Capacitive Sensors for Soft Systems," *Adv. Mater. Technol.*, pp. n/a–n/a, 2017.

[21] Peregrine. (2017, Jun). [Online]. Available: theperegrine.com